Title: Thyroid status regulates tumor microenvironment delineating breast cancer fate

Helena Andrea Sterle[1], Ximena Hildebrandt[1], Matías Valenzuela Álvarez[2], María Alejandra Paulazo[1], Luciana Mariel Gutierrez[2], Alicia Juana Klecha[1], Florencia Cayrol[1], María Celeste Díaz Flaqué[1], Cinthia Rosemblit[1], María Laura Barreiro Arcos[1], Lucas Colombo[3], Marcela Fabiana Bolontrade[2], Vanina Araceli Medina[4], Graciela Alicia Cremaschi[1]

[1] Neuroimmunomodulation and Molecular Oncology Laboratory, Institute for Biomedical Research (BIOMED), School of Medical Sciences, Pontifical Catholic University of Argentina (UCA), and the National Scientific and Technical Research Council (CONICET), Av. Alicia Moreau de Justo 1600, C1107AFF, Buenos Aires, Argentina.

[2] Remodeling Processes and Cellular Niches Laboratory, Institute of Translational Medicine and Biomedical Engineering (IMTIB), National Scientific and Technical Research Council (CONICET), Italian Hospital of Buenos Aires and the University Institute of the Italian Hospital (IUHI), Tte. Gral. Juan D. Perón 4190, C1199ABB, Buenos Aires, Argentina.

[3] Immunobiology Department, Investigation Area, Institute of Oncology Angel H. Roffo, University of Buenos Aires (UBA), National Scientific and Technical Research Council (CONICET), Av. San Martín 5481, C1417DTB, Buenos Aires, Argentina.

[4] Laboratory of Tumor Biology and Inflammation, Institute for Biomedical Research (BIOMED), School of Medical Sciences, Pontifical Catholic University

of Argentina (UCA), and the National Scientific and Technical Research Council (CONICET), Av. Alicia Moreau de Justo 1600, C1107AFF, Buenos Aires, Argentina.

Corresponding author

Graciela Alicia Cremaschi, PhD.

Neuroimmunomodulation and Molecular Oncology Laboratory

Institute for Biomedical Research (BIOMED), School of Medical Sciences, Pontifical Catholic University of Argentina (UCA), and the National Scientific and Technical Research Council (CONICET)

Av. Alicia Moreau de Justo 1600, 3rd floor, C1107AFF, Buenos Aires, Argentina.

Phone: +54 11 4349 0200 ext. 1236

e-mail: graciela_cremaschi@uca.edu.ar; gacremaschi@gmail.com

Short title: Thyroid status and breast cancer progression

Key words: breast cancer, hypothyroidism, hyperthyroidism, antitumor immunity, mesenchymal stem cells.

Word count: 5518

Abstract

The patient's hormonal context plays a crucial role in the outcome of cancer. However, the association between thyroid disease and breast cancer risk remains unclear. We evaluated the effect of thyroid status on breast cancer growth and dissemination in an immunocompetent mouse model. For this, hyperthyroid and hypothyroid Balb/c mice were orthotopically inoculated with triple negative breast cancer 4T1 cells. Tumors from hyperthyroid mice showed increased growth rate and an immunosuppressive tumor microenvironment, characterized by increased IL-10 levels and decreased percentage of activated cytotoxic T cells. On the other hand, a delayed tumor growth in hypothyroid animals was associated with increased tumor infiltration of activated $CD8^+$ cells and a high IFNγ/IL-10 ratio. Paradoxically, hypothyroid mice developed a higher number of lung metastasis than hyperthyroid animals. This was related to an increased secretion of tumor CCL2 and an immunosuppressive systemic environment, with increased proportion of regulatory T cells and IL-10 levels in spleens. A lower number of lung metastasis in hyperthyroid mice was related to the reduced presence of mesenchymal stem cells in tumors and metastatic sites. These animals also exhibited decreased percentages of regulatory T lymphocytes and myeloid-derived suppressor cells in spleens, but increased activated $CD8^+$ cells and IFNγ/IL-10 ratio. Therefore, thyroid hormones modulate the cellular and cytokine content of the breast tumor microenvironment. The better understanding of the mechanisms involved in these effects could be a starting point for the discovery of new therapeutic targets for breast cancer.

Introduction

Breast cancer is the most commonly diagnosed cancer worldwide, accounting for almost 25% cancer cases among women, and is the leading cause of cancer death in over 100 countries (Bray *et al.* 2018). In spite of representing only 15-20% of breast carcinomas, triple negative breast cancer (TNBC) is highly relevant as there are no specific therapies for this subgroup, thus having a poorer prognosis than other breast cancer types (Li *et al.* 2018). However, TNBC show a higher degree of stromal and intratumoral infiltrating lymphocytes, which turned them into an interesting target for immunotherapy although they have been originally considered poorly immunogenic due to their low rate of mutations (García-Teijido *et al.* 2016; Vikas *et al.* 2018). In addition to lymphocytes, tumor microenvironment (TME) is formed by many other cell populations, such as other immunocompetent cells, vascular endothelial cells, mesenchymal stem cells (MSC) and cancer-associated fibroblasts, as well as non-cellular constituents, including cell secreted proteins, co-factors and enzymes, cytokines and hormones, that are key regulators of tumor progression (Mizejewski 2019).

Among these factors, thyroid hormones (THs), thyroxine (T4) and triiodothyronine (T3), have been poorly studied. Although THs are essential for normal cell function, due to their role in the regulation of cell metabolism, differentiation and proliferation, the relationship between patients' thyroid status and the risk of breast cancer is not clear. While hyperthyroidism has been mostly related to an increased risk of breast cancer (Hellevik *et al.* 2009; Tosovic *et al.* 2010; Szychta *et al.* 2013; Sogaard *et al.* 2016; Weng *et al.* 2018), epidemiologic studies in hypothyroid patients are controversial. Some

95 authors have found hypothyroidism to be a risk factor for breast cancer (Smyth
96 *et al.* 1998; Kuijpens *et al.* 2005; Weng *et al.* 2018), while others indicate that it
97 protects patients from the disease (Cristofanilli *et al.* 2005; Sogaard *et al.* 2016).
98 These studies show some limitations, including the heterogeneity of thyroid
99 status evaluation, thus underestimating or overestimating the real patient
100 population, and the inclusion of patients with different thyroid pathologies, many
101 of them with autoimmune components that could differentially affect tumor
102 development and dissemination (Angelousi *et al.* 2012).

103 Both T3 and T4 have been described to induce cell proliferation and to stimulate
104 cell invasion on human breast cancer cell lines *in vitro* (Tang *et al.* 2004; Hall *et*
105 *al.* 2008; Flamini *et al.* 2017). However, their effects on other components of the
106 TME have not been studied, and could be critical for the progression of the
107 disease. In this context, we have recently shown in T-cell lymphoma tumor-
108 bearing mice that hyperthyroidism reduces the intratumoral cytotoxic activity of
109 immune cells, contributing to an increased growth rate of primary tumors (Sterle
110 *et al.* 2016). Interestingly, a higher tumor dissemination was found in
111 hypothyroid animals and this was related to regional and systemic suppression
112 of antitumor immune responses (Sterle *et al.* 2016). THs have indeed been
113 described to regulate the functionality of a great variety of immune cells,
114 affecting their chemotaxis, phagocytosis, the generation of reactive oxygen
115 species and the production of cytokines (Jara *et al.* 2017; Montesinos & Pellizas
116 2019). Increased TH levels induce pro-inflammatory response amplification in
117 neutrophils, macrophages and dendritic cells (van der Spek *et al.* 2017;
118 Montesinos & Pellizas 2019) and affect the activity of NK cells and T and B cell
119 mediated responses as well (DeVito *et al.* 2011). The role of immune cells in

tumor progression depends on many factors including cell type, their location, density and phenotype, as well as the secreted cytokines and chemokines (Pottier *et al.* 2015). In breast cancer, a high number of tumor infiltrating $CD8^+$ T lymphocytes and B lymphocytes has been associated with a favorable prognosis (Mahmoud *et al.* 2011; Linnebacher & Maletzki 2012). On the contrary, the most aggressive breast tumor phenotypes show increased frequencies of regulatory T lymphocytes (Tregs) (Plitas *et al.* 2016). Also the peripheral blood levels of myeloid-derived suppressor cells (MDSC) correlate with breast cancer development and have been proposed as biomarkers for this disease (Markowitz *et al.* 2013).

Recent research has also shown that THs can modulate the recruitment and invasion of MSC to tumors in hepatocellular murine carcinoma (Schmohl *et al.* 2015, 2019). These multipotent stem cells are important components of TME and are mainly found in bone marrow, adipose tissue and dental pulp. They can migrate and interact with tumor cells at different stages of tumor progression, where both tumor-promoting and tumor-suppressive effects have been described (Ridge *et al.* 2017). In breast cancer, the presence of MSC has been principally related to increased tumor progression and metastasis (Karnoub *et al.* 2007; Maffey *et al.* 2017; Melzer *et al.* 2018).

On this basis, the aim of this study was to evaluate the effect of thyroid status on breast cancer growth and dissemination in an immunocompetent mouse model, analyzing its impact on TME that could importantly contribute to the progression of the disease. We here show that THs not only induce breast cancer cell proliferation, but they also regulate the distribution of

144 immunocompetent cells and MSC within the TME, as well as the secretion of
145 cytokines, thus influencing metastatic dissemination.

146

147 ## Materials and methods

148 ### *Animal models*

149 Murine models of hyperthyroidism or hypothyroidism were developed using
150 female Balb/c mice, 6–8 weeks old, that were bred and kept at the Institute for
151 Biomedical Research (BIOMED, Argentina) in accordance with the ARRIVE
152 Guidelines (Kilkenny *et al.* 2010). All experimental protocols were approved by
153 the Institutional Committee for the Care and Use of Laboratory Animals,
154 BIOMED. Hyperthyroid mice were obtained by daily administration of L-
155 thyroxine (T4; 0.0012% w/v; Sigma-Aldrich, MO, USA) in the drinking water for
156 28 days (Sterle *et al.* 2016). To induce hypothyroidism, the drinking water was
157 supplemented with the antithyroid drug propylthiouracil (PTU; 0.05% w/v;
158 Sigma-Aldrich) for 14 days (Klecha *et al.* 2006; Sterle *et al.* 2014, 2016). At
159 these time points mice were inoculated with breast cancer cells and hormonal
160 treatments were maintained until the end of the experiments.

161 ### *Breast cancer model*

162 To generate solid tumors, euthyroid, hyperthyroid or hypothyroid mice were
163 inoculated orthotopically in the abdominal mammary gland with 1×10^5
164 syngeneic breast cancer 4T1 cells (ATCC CRL-2539) in serum-free phosphate-
165 buffered saline (PBS), as described (Pulaski & Ostrand-Rosenberg 2001; Sterle
166 *et al.* 2019). Tumor length and width were measured every 2 to 4 days using

calipers, and tumor volume was calculated as $V = \pi/ 6 \times length \times width^2$ (Sterle *et al.* 2016, 2019). After 21 or 35 days, mice were sacrificed, and tissues were removed and weighted. To determine the spontaneous metastatic dissemination, lungs were fixed in 3.7% v/v paraformaldehyde and the number of tumor *foci* was counted. For the experimental metastasis test, mice were inoculated through the tail vein with 1×10^5 4T1 cells and after 35 days they were sacrificed, and lung tumor *foci* were counted.

Flow cytometry for immunophenotyping

Single cell suspensions obtained from tumors, tumor draining lymph nodes and spleens were stained with antibodies against various cell surface markers using standard staining methods. The panel of commercially available and fluorochrome conjugated anti-mouse monoclonal antibodies that were used in the study are shown in **Supplementary Table 1**. Samples were run on a BD Accuri C6 flow cytometer (BD Biosciences, CA, USA) and data was analyzed using the FlowJO or the BD Accuri C6 software (both from BD Biosciences).

Intracellular FoxP3 staining

After surface staining, single cell suspensions were fixed with the *Mouse Foxp3 Fixation Buffer* (BD Biosciences) and permeabilized at 37 ºC for 30 min with the *Mouse Foxp3 Permeabilization buffer* (BD Biosciences) following manufacturers' instructions. Cells were then incubated with the FoxP3 antibody **(Supplementary Table 1)** for 40 min at room temperature. After washing with PBS, the percentage of $CD25^+$ $FoxP3^+$ events was determined by flow cytometry within the gated population of $CD4^+$ cells.

Isolation and culture of bone marrow derived MSC

Primary MSC cultures were established from mouse bone marrow (BM) cells obtained from the hind femurs and tibias of 5-week-old Balb/c mice. The bones were aseptically removed, dissected clean of attached muscles, and flushed with PBS. Cells were then washed with PBS and suspended in Dulbecco's Modified Eagle Medium (DMEM) supplemented with 10% v/v FBS. BM cells (1×10^7/ml) were placed in 75-cm^2 tissue culture flasks and incubated at 37°C. After 3 days, non-adherent cells were removed, and fresh culture medium was added. Four weeks later, an aliquot of cells was differentiated into osteoblasts, adipocytes and chondroblasts (Bolontrade *et al.* 2012) and phenotyped as MSC by flow cytometry as Sca-1^+, $CD105^+$, $CD44^+$, $CD45^-$ $CD11b^-$ and MHC-II^- using specific antibodies.

In vitro MSC migration assays

For the *in vitro* migration studies, tumor conditioned media (CM) were obtained by mincing tumors from eu-, hyper- or hypothyroid mice into 1 mm^2 fragments, that were then incubated in DMEM for 24 h. Migratory response of cultured MSC to this CM as chemoattractant was assayed for 4 h at 37 °C using a modified Boyden Chamber (Neuro Probe, Inc., MD, USA). For this, a suspension of 1.2×10^4 MSC in 50 µl PBS was seeded on the upper wells and 28 µl of each CM were added in triplicate into the lower wells. The migration through an 8 µm pore polycarbonate filter (Nucleopore membrane; Neuro Probe) was evaluated after 4 h. For this, the filter was carefully removed and cells on the upper side were scraped off. Cells attached to the lower side of the filter were fixed in 2% paraformaldehyde and stained with 4′,6-Diamidino-2-

phenylindole dihydrochloride (Sigma-Aldrich). Cells were counted using fluorescent-field microscopy. Images captured in 3 representative visual fields were quantified using Image J software (NIH, National Institutes of Health), and the mean number of nuclei/field ± SEM was calculated (Bolontrade *et al.* 2012).

In vivo MSC migration

For *in vivo* migration studies, firefly luciferase stably transfected 4T1 (4T1-fluc) cells were inoculated in eu-, hyper- or hypothyroid mice as described before. At day 28 post-inoculation (p.i.) MSC stained with 1,1′-dioctadecyl-3,3,3′,3′-tetramethylindotricarbocyanine iodide (DiR) (Molecular Probes, Life technologies, OR, USA) were injected intravenously (i.v.) through the tail vein at 5×10^5 cells in 0.2 ml PBS. On day 35 p.i. mice were injected intraperitoneally with D-luciferin solution (150 mg/kg, Sigma-Aldrich). DiR *in vivo* tracking on isolated tissues was followed with Fluorescence Imaging (FI) IVIS Lumina Bioluminometer (Xenogen, CA, USA). Captured images were analyzed by measuring the region of interest and results expressed as average photons per second per square centimeter per steradian (p/sec/cm^2/sr) (Bolontrade *et al.* 2012).

Statistical analysis

The means of the different experimental groups were analyzed for statistical significance using GraphPad PRISM 7.0 version for Windows (GraphPad Software, Inc., CA, USA). One-way ANOVA followed by Tukey's post hoc analysis was used to assess statistical significance. The differences between

the means were considered significant if $p<0.05$. The results are expressed as mean ± SEM.

Additional methods are described in Supplementary Materials and Methods.

RESULTS

Tumor growth and dissemination are modulated by thyroid status

To evaluate the effect of the thyroid status on breast cancer development, we analyzed the tumor volume and metastatic dissemination on euthyroid (control), hyperthyroid, and hypothyroid mice bearing 4T1 TNBC tumors. Hyperthyroid mice showed an increased tumor growth rate that became significant at day 21 p.i. **(Figure 1A)**. The tumor weight of hyperthyroid mice was also higher at that time, compared to the other two groups **(Figure 1B)**. However, no visible metastasis could be detected at this time point in any mouse (data not shown). At day 35 p.i. the tumor volume and weight of hypothyroid tumors was significantly decreased compared to euthyroid mice, thus indicating a slower growth rate of these tumors **(Figure 1A-C)**. In spite of the later results, the number of lung metastasis was increased in hypothyroid mice at this time point **(Figure 1D,E)**. Also, in an experimental metastasis test, where 4T1 cells were intravenously inoculated into eu-, hyper- or hypothyroid mice, an increased number of lung metastasis was detected in hypothyroid mice at day 35 p.i. **(Figure 1F)**. Similar results were obtained with the LM3 mammary carcinoma cell line growing *in vivo* in mice with different thyroid status **(Supplementary Figure 1)**.To confirm the thyroid status of the experimental animals, serum

levels of T3, T4 and TSH were measured at the end of each experiment **(Figure 1G)**.

Histopathological analysis of H&E-stained tissue sections from tumors 35 days p.i. indicated that all tumors were highly undifferentiated with high nuclear polymorphism **(Figure 2A)**. However, tumors from hypothyroid mice exhibited an increased percentage of necrotic areas compared to control and hyperthyroid ones **(Figure 2A-B)**. These tumors also displayed a decreased percentage of PCNA-positive cells per field compared to tumors from control and hyperthyroid mice **(Figure 2A-B)**.Tissue sections showed a very low number of apoptotic cells, which was similar in all three experimental groups **(Figure 2A-B)**.

To additionally elucidate the mechanisms involved in the effects of thyroid status on tumor growth, we analyzed the direct action of THs on 4T1 cell proliferation. For this, 4T1 cells were treated *in vitro* with the combination of T3 and T4, as found in circulation, at physiologic (T3 $1x10^{-9}$ mol/L, T4 $1x10^{-7}$ mol/L) or supraphysiologic (T3 $1x10^{-8}$ mol/L and T4 $1x10^{-6}$ mol/L) concentrations. However, only supraphysiologic concentrations of THs increased the proliferation of breast cancer cells **(Figure 2C-E)**.

Thyroid status modulates the tumor infiltration of immune cells

Despite the proliferative action of supraphysiologic levels of THs on 4T1 cells, there are many other factors that could outline the progression of tumors growing *in vivo* in syngeneic animals. The importance of the immune system in the TME of breast cancer is increasingly being recognized. Therefore, the effect

of thyroid status on the composition of the immune cell infiltration in 4T1 tumors was evaluated by flow cytometry. The presence of tumor infiltrating lymphocytes (TILs) was first determined by the forward and side scatter analysis of tumor cell suspensions from eu-, hyper- and hypothyroid mice. Tumors that were excised from hyperthyroid mice 21 days after 4T1 cell inoculation showed a decreased percentage of TILs, while this percentage was significantly increased in tumors from hypothyroid mice at day 35 p.i. **(Figure 3A,B)**. A further analysis of the infiltrating immune subsets within the gated TILs population showed no differences in the percentage of NK cells, B lymphocytes or $CD4^+$ and $CD8^+$ T cells **(Figure 3C-F)**. However, 21-day tumors from hyperthyroid mice showed a reduced percentage of activated $CD8^+$ T cells that were detected with the CD44 marker **(Figure 3G)**. On the other hand, the levels of activated $CD8^+$ T lymphocytes were increased in both 21- and 35-day tumors from hypothyroid mice **(Figure 3G)**. These differences in the activation levels of $CD8^+$ T lymphocytes could be related to the modulation of immunosuppressive cells within the TIL population induced by THs. However, no Tregs could be detected within the TILs gated population and the percentage of MDSC was similar between the three groups **(Figure 3H)**.

Both tumor and immunocompetent cells can secrete cytokines and chemokines that shape the TME and orchestrate tumor growth and metastatic dissemination. Although IFNγ, IL-10 and TNF-α, mainly produced by immune cells, are important regulators of tumor development, their role in breast cancer is controversial both as tumor promoters and inhibitors. For this reason, we measured the production of these cytokines in the CM obtained from 21-day tumors from eu-, hyper- or hypothyroid mice. Tumors from hypothyroid mice

showed increased secretion levels of IFNγ compared to tumors from hyperthyroid animals **(Figure 4A)**. On the contrary, the IL-10 levels were only increased in the CM obtained from hyperthyroid mice **(Figure 4B)**. Thus, the ratio between IFNγ and IL-10 levels was increased in hypothyroid mice when compared to euthyroid ones and this difference was even more significant when compared to hyperthyroid animals **(Figure 4C)**. However, the tumors from all three experimental groups showed similar production levels of TNF-α **(Figure 4D)**. The chemokine CCL2, mostly produced by tumor cells and overexpressed in TNBC, is related to cancer invasiveness and metastasis (Dutta *et al.* 2018). The levels of this chemokine were increased in tumor CM from hypothyroid mice in comparison with the euthyroid group and this difference was even greater when compared with tumors from hyperthyroid animals **(Figure 4E)**.

Thyroid status modulates systemic immune responses

As an indication of the modulation of the systemic immunity by the thyroid status, the distribution of splenic immune subsets was also analyzed. Flow cytometry analysis of immune suspensions obtained from spleens from 21-day tumor bearing mice show increased percentages of NK cells in hyperthyroid mice **(Figure 5A)**. The percentage of B lymphocytes was similar in all three groups at this time point **(Figure 5B)**. However, a decreased percentage of total $CD8^+$ cells, but not in the frequencies of $CD8^+CD44^+$ lymphocytes could be detected **(Figure 5C,D)**. These variations in spleen immune cell distributions were accompanied by a decrease in the percentages of immunosuppressive MDSC **(Figure 5E)**. In spleens from 35-day tumor bearing mice, however, there were no differences in the percentages of NK cells **(Figure 5A)**, but the

percentage of B lymphocytes was increased in hypothyroid mice. Spleens from hyperthyroid mice showed an increased proportion of activated $CD8^+$ cells **(Figure 5D),** but decreased frequencies of Tregs when compared to hypothyroid mice **(Figure 5F)**. Additionally, the splenocytes from hyperthyroid mice that were re-stimulated *in vitro* with irradiated 4T1 cells produced increased levels of IFNγ **(Figure 5G)**. On the other hand, the production of IL-10 was increased in spleens from hypothyroid mice **(Figure 5H)** and therefore the ratio between IFNγ and IL-10 splenic levels was increased in hyperthyroid mice and decreased in hypothyroid ones **(Figure 5I)**.

Additionally, the distribution of immune subsets in the regional tumor-draining lymph nodes (TDLN) from hypothyroid mice show a more immunosuppressive phenotype when compared to hyperthyroid ones, with an increased proportion of $CD4^+$ and $CD8^+$ T lymphocytes, but also increased percentages of Tregs, leading to a decreased percentage of activated $CD8^+$ T cells **(Supplementary Figure 2)**.

Hyperthyroidism inhibits the migration of MSC to 4T1 tumors and metastasis

The production of CCL2 is related to metastasis formation and has also been related to MSC homing to tumors (Dwyer *et al.* 2007). Once they are incorporated into the tumor, MSC can differentiate into fibroblasts, pericytes or tumor-associated fibroblasts and through the secretion of cytokines can affect the tumor and the immune cells (Bergfeld & DeClerck 2010). Therefore, we evaluated the presence of MSC in the 4T1 tumors from control, hyper- and hypothyroid mice. Because of the lack of MSC specific markers that would

unequivocally distinguish MSC from other mesenchymal–lineage cells within the TME in this syngeneic model, pre-stained MSC were administered into tumor-bearing mice in order to visualize and track the *in vivo* migratory and tumor homing behavior of MSC. For this, eu-, hyper- and hypothyroid mice were first orthotopically inoculated with 4T1-fluc cells and after 28 days they received an intravenous inoculation of DiR-stained MSC. One week later, animals were treated with luciferin and organs were excised to be analyzed by *ex vivo* imaging. This allowed us to detect the fluorescent signal associated to those MSC that were able to home into the primary tumor site and into the metastasis that showed luciferase activity. It is worth noting that given the doubling time of MSC (approximately 3-5 days) the fluorescent signal of the pre-stained cells was not lost until the experimental end-point. Tumors from hyperthyroid mice showed a decreased fluorescence intensity of DiR when compared to the other experimental groups, thus indicating a reduced migration of MSC to these tumors **(Figure 6A,B)**. Likewise the fluorescence intensity of DiR in lungs of hyperthyroid mice was also decreased **(Figure 6C,D)**, suggesting a decreased migration of MSC also to metastatic nodules. To further investigate how thyroid status regulates the migration and invasiveness of MSC into tumors, CM from tumors grown in eu-, hyper- and hypothyroid mice were used to evaluate the migration of MSC *in vitro*, using a Boyden chamber assay. The migration of MSC towards the CM from 35-day tumors from hyperthyroid mice was decreased **(Figure 6E)**. Likewise, the CM of lungs from 35-day tumor-bearing hyperthyroid mice showed decreased MSC migration **(Figure 6F)**. As an approach to evaluate the differentiation capacity of MSC once they are recruited into the TME, MSC were cultured *in vitro* during 7 days with 10% CM from

tumors grown in eu-, hyper- and hypothyroid mice. The area of individual cells was evaluated as an indicative of cells that are undergoing a differentiation process (Álvarez *et al.* 2020). MSC cultured with the supplementation of CM from tumors from both eu- and hypothyroid animals, but not from hyperthyroid ones, showed increased cell areas compared to MSC cultured without the addition of CM (basal) **(Figures 6 G,H)**, thus indicating that the TME from eu- and hypothyroid mice have a higher differentiating potential on MSC than hyperthyroid ones.

Discussion

As components of TME, THs affect tumor biology. In fact, our results show a dual effect of thyroid status on breast cancer growth and dissemination. The growth rate of 4T1 primary tumors is increased in hyperthyroid mice and slightly decreased in hypothyroid ones, but the formation of metastasis is enhanced in hypothyroid conditions. We here tried to unravel some of the possible cellular and molecular mechanisms involved in these opposite effects, that would explain some contradictory results on the impact of thyroid status in breast cancer incidence and progression (Tosovic *et al.* 2010; Sogaard *et al.* 2016; Weng *et al.* 2018).

THs seem to have a direct effect on 4T1 cell growth as the treatment of these cells with supraphysiologic levels of THs *in vitro* induce their proliferation. Indeed, several authors have previously described a direct proliferative effect of THs on breast cancer cell lines. Both T3 and T4 can induce the activation of the estrogen receptor (ER) in MCF-7 and T47-D cells, leading to enhanced proliferation (Tang *et al.* 2004; Hall *et al.* 2008). THs can also stimulate the

proliferation of the TNBC MDA-MB-231 cells through non-genomic mechanisms that regulate the expression of survival-related genes (Glinskii *et al.* 2009). In contrast, a retarded primary tumor growth has been described in hypothyroid nude mice bearing MDA-MB-468 TNBC xenografts but, in accordance to our results, these animals exhibited enhanced tumor cell invasion and metastasis formation (Martínez-Iglesias *et al.* 2009). Similarly to our results that show a decreased percentage of PCNA-positive cells and increased necrosis in tumors from hypothyroid mice, tumors from nude hypothyroid mice bearing MDA-MB-468 TNBC xenografts also exhibited a decreased percentage of Ki67-positive cells and increased necrotic areas. These effects were described to be independent from the expression of thyroid receptors in the tumor cells and were associated to the modulation by THs of the function of tumor stromal cells (Martínez-Iglesias *et al.* 2009). Therefore, thyroid status modulation of breast cancer progression could be related to both a direct action of THs on tumor cells and an indirect effect, modulating different components of the TME.

Our results indeed indicate that the composition of 4T1 TME is modulated by the thyroid status. First, tumors from animals with different circulating levels of THs show different infiltration of immunocompetent cells. In 21-day tumors from hyperthyroid animals there is a decreased percentage of total TILs. Moreover, these tumors exhibit a decreased percentage of activated $CD8^+$ T lymphocytes and increased secretion levels of IL-10, thus suggesting that hyperthyroidism promotes a local immunosuppressive milieu, which could contribute to the growth of the primary tumor. Similarly, we have previously described in hyperthyroid T-cell lymphoma tumor-bearing mice an increased tumor growth rate, associated to reduced TILs and a decreased percentage of infiltrating

428 $CD8^+$ lymphocytes (Sterle *et al.* 2016). On the contrary, 35-day tumors from
429 hypothyroid animals showed an increased percentage of TILs accompanied by
430 a higher proportion of activated cytotoxic $CD8^+$ cells and increased secretion of
431 IFNγ. Therefore, the deficiency of THs leads to an enhanced cytotoxic
432 microenvironment that could contribute to the decreased primary tumor size in
433 hypothyroid mice. The intratumoral levels of IFNγ may not only shape immune
434 responses but might also directly affect tumor cell behavior and survival in a
435 large part of the tumor mass (Hoekstra *et al.* 2020). Indeed, even very low
436 amounts of IFNγ in the TME have been described to affect the phenotype,
437 growth and metastasis of 4T1 tumors (DuPre' *et al.* 2008).

438 The tumors from hypothyroid mice also showed increased CCL2 levels, which
439 could contribute to the enhanced metastatic potential of these tumors. In
440 patients with breast carcinoma, high circulating levels of this chemokine as well
441 as increased production of CCL2 within the TME have been associated with
442 poor prognosis (Li *et al.* 2013). Moreover, the treatment of different human
443 breast cancer cell lines with CCL2 induces cell invasion, without affecting cell
444 proliferation (Dutta *et al.* 2018). This chemokine can be secreted by both tumor
445 and stromal cells. In an *in vivo* model of 4T1 breast cancer, the CCL2 produced
446 by the stromal cells of primary tumors has been described to promote lung
447 metastasis, while tumor cell-derived CCL2 contributes to the invasiveness once
448 tumor cells enter the circulation (Yoshimura *et al.* 2013). The mechanism of
449 action of CCL2 in breast cancer is still not fully understood. It has been shown
450 to induce the expression of epithelial to mesenchymal transition (EMT) markers
451 (Dutta *et al.* 2018) and has been involved in the development and mobilization

of endothelial precursor cells, which can contribute to tumor neovascularization (Chen *et al.* 2016).

CCL2 has also been described to induce the migration of human and murine BM-MSC, both *in vitro* and *in vivo* (Dwyer *et al.* 2007; Boomsma & Geenen 2012). Moreover, the migration of BM-MSC to breast tumors has been widely described and has also been associated to metastasis formation (Hill *et al.* 2020). The mechanisms involved in the promotion of metastasis by MSC remain unclear. Even though BM-MSC have been described to migrate and form clusters in pre-metastatic sites before the arrival of tumor cells (Kaplan *et al.* 2005), many authors have described that the cell to cell contact with tumor cells induces their migration. In breast cancer, MSC can stimulate tumor cell migration through a paracrine signaling mediated by the hypoxia inducible factor (Chaturvedi *et al.* 2013) and facilitating the EMT (Martin *et al.* 2010). MSC have also been shown to fuse with breast cancer cells, contributing to tumor heterogeneity and thus increasing their metastatic potential (Melzer *et al.* 2018). We therefore evaluated the effect of thyroid status on MSC migration into 4T1 tumors. Because of the lack of unique MSC specific markers, we were not able to directly detect MSC in 4T1 tissues. The most commonly used markers for MSC could also stain other mesenchymal-derived cells or even subsets of 4T1 cells (Matilainen *et al.* 2012). We have instead inoculated pre-stained BM-MSC into mice with already established tumors in order to track their migration into primary tumors and metastasis, as an indicator of what is endogenously occurring. Hyperthyroid mice showed a decreased recruitment of pre-stained MSC to both tumors and metastasis in comparison to control and hypothyroid mice. Accordingly, the *in vitro* migration assay showed a decreased migration of

MSC towards the hyperthyroid tumor CM, thus suggesting that the thyroid status modulates endocrine and paracrine signals produced by tumor cells and other TME components that are involved in MSC recruitment to tumors, which may include CCL2. Moreover, MSC incubated with hyperthyroid- derived tumor CM showed less differentiation capacity than the ones cultured in the presence of tumor CM from eu- or hypothyroid mice, as it was evaluated through the analysis of MSC morphology. Within the tumor, MSC can differentiate into fibroblasts, pericytes or tumor-associated fibroblasts, which are also involved in the promotion of metastasic spread of breast cancer (Hill *et al.* 2020). Contrary to our observations, the treatment of human MSC with T3 or T4 in the presence of hepatocellular carcinoma cell-CM induced their migration (Schmohl *et al.* 2015). Also, in an *in vivo* xenograft model, the induction of hyperthyroidism after the inoculation of the human hepatocellular carcinoma cell line HuH7 showed increased recruitment of MSC to tumors compared to euthyroid and hypothyroid mice, which was associated to a direct action of THs on MSC, mediated by their membrane receptor, the integrin αvβ3 (Schmohl *et al.* 2015, 2019). These different effects of THs on BM-MSC migration could be associated either to the tumor type or the time point (21 days after tumor injection) when hyperthyroidism is established. In breast cancer, the regulation of CCL2 production by THs could be involved in this phenomenon, but further investigations should be performed to unravel all the mechanisms by which the thyroid status regulates MSC recruitment to breast tumors and how this affects the formation of metastasis.

In previous studies performed in a murine T-cell lymphoma model we have shown that THs can affect the formation of metastasis through the modulation

of systemic antitumor immune responses (Sterle *et al.* 2016). Immune responses involve coordination across different cell types and tissues, thus the regulation of the distribution of immune subsets in secondary lymphoid organs is crucial for effective antitumor immunity (Spitzer *et al.* 2017). Our results show a more immunosuppressive phenotype of spleens from hypothyroid mice compared to control and hyperthyroid ones. Already at 21 days p.i. hypothyroid spleens exhibit decreased NK percentages compared to hyperthyroid animals. Moreover, 35 days p.i. spleens from hypothyroid mice show an increased percentage of Tregs that probably leads to the decreased proportion of activated $CD8^+$ T cells and decreased IFNγ/IL-10 ratio that is observed. Therefore, hypothyroidism induces a tolerogenic phenotype in spleens and TDLN, which is likely to contribute to the increased formation of metastasis in these animals. Despite the fact that the TDLN is the first place where tumor antigens are presented to the naïve immune system and is critical for the activation of antitumor immunity (Munn & Mellor 2006), the microenvironment of the TDLN is frequently immunosuppressed in cancer patients and it often mediates tumor cell migration and metastasis formation (Chandrasekaran & King 2014). Indeed in our model, TDLNs from hypothyroid mice exhibit a more immunosuppressive milieu compared to the other experimental groups, with an increased proportion of Tregs and decreased percentage of activated $CD8^+$ cells, which could facilitate the dissemination of tumor cells. These results could be related to a direct effect of THs on immune cells as we have previously demonstrated that the thyroid status modulates the T cell reactivity after antigen or polyclonal-activation that is up-regulated in hyperthyroid animals and down-regulated in hypothyroid ones (Klecha *et al.* 2000, 2006).

Based on these results, we conclude that there is a complex regulation of breast cancer progression by thyroid status that would account for the controversial results shown in the literature. THs directly regulate tumor cell proliferation, but they also affect the cellular and cytokine content of the TME and the systemic immunity. This work strengthens the importance of screening thyroid status in breast cancer patients to ensure euthyroid conditions that would impair both exacerbated tumor growth and metastatic dissemination. Interestingly, a recent uncontrolled clinical study has shown that euthyroid hypothyroxinemia, a therapeutic setting in which T3 replaces host circulating T4, achieves the arrest of breast cancer and other solid tumors growth (Hercbergs *et al.* 2015). Therefore, further unraveling the mechanisms involved in the paradoxical effects of THs in breast cancer and the role of the different TH receptors in each cell type of the TME, could lead to a better understanding of the association between breast cancer and thyroid diseases and could be a starting point for the discovery of new therapeutic targets.

Declaration of interest

The authors declare that there is no conflict of interest that could be perceived as prejudicing the impartiality of the research reported.

Funding

This work was supported by the National Agency for Scientific and Technological Promotion (ANPCYT, PICT 2015-0874 and PICT 2018-3703), the National Cancer Institute (Grant for Basic Research Projects No. DI-2018-19-

549 APN-INC#MS/2018) and the National Scientific and Technical Research
550 Council (PIP-CONICET 11220150100503CO).

551

552 **References**

553 Álvarez MV, Gutiérrez LM, Auzmendi J, Correa A, Lazarowski A & Bolontrade
554 MF 2020 Acquisition of stem associated-features on metastatic
555 osteosarcoma cells and their functional effects on mesenchymal stem cells.
556 *Biochimica et Biophysica Acta - General Subjects* **1864** 129522.
557 (doi:10.1016/j.bbagen.2020.129522)
558 Angelousi AG, Anagnostou VK, Stamatakos MK, Georgiopoulos GA &
559 Kontzoglou KC 2012 Mechanisms in endocrinology: primary HT and risk for
560 breast cancer: a systematic review and meta-analysis. *European Journal of*
561 *Endocrinology* **166** 373–381. (doi:10.1530/EJE-11-0838)
562 Bergfeld SA & DeClerck YA 2010 Bone marrow-derived mesenchymal stem
563 cells and the tumor microenvironment. *Cancer and Metastasis Reviews* **29**
564 249–261. (doi:10.1007/s10555-010-9222-7)
565 Bolontrade MF, Sganga L, Piaggio E, Viale DL, Sorrentino MA, Robinson A,
566 Sevlever G, García MG, Mazzolini G & Podhajcer OL 2012 A Specific
567 Subpopulation of Mesenchymal Stromal Cell Carriers Overrides Melanoma
568 Resistance to an Oncolytic Adenovirus. *Stem Cells and Development* **21**
569 2689–2702. (doi:10.1089/scd.2011.0643)
570 Boomsma RA & Geenen DL 2012 Mesenchymal Stem Cells Secrete Multiple
571 Cytokines That Promote Angiogenesis and Have Contrasting Effects on
572 Chemotaxis and Apoptosis. *PLoS ONE* **7** e35685.
573 (doi:10.1371/journal.pone.0035685)

574 Bray F, Ferlay J, Soerjomataram I, Siegel RL, Torre LA & Jemal A 2018 Global
575 cancer statistics 2018: GLOBOCAN estimates of incidence and mortality
576 worldwide for 36 cancers in 185 countries. *CA Cancer Journal for Clinicians*
577 **68** 394–424. (doi:10.3322/caac.21492)
578 Chandrasekaran S & King MR 2014 Microenvironment of tumor-draining lymph
579 nodes: Opportunities for liposome-based targeted therapy. *International*
580 *Journal of Molecular Sciences* **15** 20209–20239.
581 (doi:10.3390/ijms151120209)
582 Chaturvedi P, Gilkes DM, Wong CCL, Kshitiz, Luo W, Zhang H, Wei H, Takano
583 N, Schito L, Levchenko A *et al.* 2013 Hypoxia-inducible factor–dependent
584 breast cancer–mesenchymal stem cell bidirectional signaling promotes
585 metastasis. *The Journal of Clinical Investigation* **123** 189.
586 (doi:10.1172/JCI64993)
587 Chen X, Wang Y, Nelson D, Tian S, Mulvey E, Patel B, Conti I, Jaen J & Rollins
588 BJ 2016 CCL2/CCR2 Regulates the Tumor Microenvironment in HER-
589 2/neu-Driven Mammary Carcinomas in Mice. *PloS One* **11** e0165595.
590 (doi:10.1371/journal.pone.0165595)
591 Cristofanilli M, Yamamura Y, Kau S-W, Bevers T, Strom S, Patangan M, Hsu L,
592 Krishnamurthy S, Theriault RL & Hortobagyi GN 2005 Thyroid hormone
593 and breast carcinoma. Primary hypothyroidism is associated with a
594 reduced incidence of primary breast carcinoma. *Cancer* **103** 1122–1128.
595 (doi:10.1002/cncr.20881)
596 DeVito P, Incerpi S, Pedersen JZ, Luly P, Davis FB & Davis PJ 2011 Thyroid
597 Hormones as Modulators of Immune Activities at the Cellular Level. *Thyroid*
598 **21** 879–890. (doi:10.1089/thy.2010.0429)

599 DuPre' SA, Redelman D & Hunter KW 2008 Microenvironment of the murine
600 mammary carcinoma 4T1: Endogenous IFN-γ affects tumor phenotype,
601 growth, and metastasis. *Experimental and Molecular Pathology* **85** 174–
602 188. (doi:10.1016/j.yexmp.2008.05.002)
603 Dutta P, Sarkissyan M, Paico K, Wu Y & Vadgama J V. 2018 MCP-1 is
604 overexpressed in triple-negative breast cancers and drives cancer
605 invasiveness and metastasis. *Breast Cancer Research and Treatment* **170**
606 477–486. (doi:10.1007/s10549-018-4760-8)
607 Dwyer RM, Potter-Beirne SM, Harrington KA, Lowery AJ, Hennessy E, Murphy
608 JM, Barry FP, O'Brien T & Kerin MJ 2007 Monocyte chemotactic protein-1
609 secreted by primary breast tumors stimulates migration of mesenchymal
610 stem cells. *Clinical Cancer Research* **13** 5020–5027. (doi:10.1158/1078-
611 0432.CCR-07-0731)
612 Flamini MI, Uzair ID, Pennacchio GE, Neira FJ, Mondaca JM, Cuello-Carrión
613 FD, Jahn GA, Simoncini T & Sanchez AM 2017 Thyroid Hormone Controls
614 Breast Cancer Cell Movement via Integrin αV/β3/SRC/FAK/PI3-Kinases.
615 *Hormones and Cancer* **8** 16–27. (doi:10.1007/s12672-016-0280-3)
616 García-Teijido P, Cabal ML, Fernández IP & Pérez YF 2016 Tumor-infiltrating
617 lymphocytes in triple negative breast cancer: The future of immune
618 targeting. *Clinical Medicine Insights: Oncology* **10** 31–39.
619 (doi:10.4137/CMO.S34540)
620 Glinskii AB, Glinsky G V, Lin H, Tang H, Sun M, Davis FB, Luidens MK, Mousa
621 SA, Hercbergs AH & Davis PJ 2009 Modification of survival pathway gene
622 expression in human breast cancer cells by tetraiodothyroacetic acid (
623 tetrac). *Cell Cycle* **8** 3562–3570. (doi:10.4161/cc.8.21.9963)

624 Hall LC, Salazar EP, Kane SR & Liu N 2008 Effects of thyroid hormones on
625 human breast cancer cell proliferation. *The Journal of Steroid Biochemistry*
626 *and Molecular Biology* **109** 57–66. (doi:10.1016/j.jsbmb.2007.12.008)
627 Hellevik AI, Asvold BO, Bjoro T, Romundstad PR, Nilsen TIL & Vatten LJ 2009
628 Thyroid Function and Cancer Risk: A Prospective Population Study.
629 *Cancer Epidemiology Biomarkers & Prevention* **18** 570–574.
630 (doi:10.1158/1055-9965.EPI-08-0911)
631 Hercbergs A, Johnson RE, Ashur-Fabian O, Garfield DH & Davis PJ 2015
632 Medically Induced Euthyroid Hypothyroxinemia May Extend Survival in
633 Compassionate Need Cancer Patients: An Observational Study. *The*
634 *Oncologist* **20** 72–76. (doi:10.1634/theoncologist.2014-0308)
635 Hill BS, Sarnella A, D'Avino G & Zannetti A 2020 Recruitment of stromal cells
636 into tumour microenvironment promote the metastatic spread of breast
637 cancer. *Seminars in Cancer Biology* **60** 202–213.
638 (doi:10.1016/j.semcancer.2019.07.028)
639 Hoekstra ME, Bornes L, Dijkgraaf FE, Philips D, Pardieck IN, Toebes M,
640 Thommen DS, van Rheenen J & Schumacher TNM 2020 Long-distance
641 modulation of bystander tumor cells by CD8+ T-cell-secreted IFN-γ. *Nature*
642 *Cancer* **1** 291–301. (doi:10.1038/s43018-020-0036-4)
643 Jara EL, Muñoz-Durango N, Llanos C, Fardella C, González PA, Bueno SM,
644 Kalergis AM & Riedel CA 2017 Modulating the function of the immune
645 system by thyroid hormones and thyrotropin. *Immunology Letters* **184** 76–
646 83. (doi:10.1016/j.imlet.2017.02.010)
647 Kaplan RN, Riba RD, Zacharoulis S, Bramley AH, Vincent L, Costa C,
648 MacDonald DD, Jin DK, Shido K, Kerns SA *et al.* 2005 VEGFR1-positive

haematopoietic bone marrow progenitors initiate the pre-metastatic niche. *Nature* **438** 820–827. (doi:10.1038/nature04186)

Karnoub AE, Dash AB, Vo AP, Sullivan A, Brooks MW, Bell GW, Richardson AL, Polyak K, Tubo R & Weinberg RA 2007 Mesenchymal stem cells within tumour stroma promote breast cancer metastasis. *Nature* **449** 557–563. (doi:10.1038/nature06188)

Kilkenny C, Browne W, Cuthill I, Emerson M & Altman D 2010 Improving bioscience research reporting: The ARRIVE guidelines for reporting animal research. *Journal of Pharmacology and Pharmacotherapeutics* **1** 94. (doi:10.4103/0976-500X.72351)

Klecha AJ, Genaro AM, Lysionek AE, Caro RA, Coluccia AG & Cremaschi GA s. l. 2000 Experimental evidence pointing to the bidirectional interaction between the immune system and the thyroid axis. *International Journal of Immunopharmacology* **22** 491–500.

Klecha AJ, Genaro AM, Gorelik G, Barreiro Arcos ML, Silberman DM, Schuman M, Garcia SI, Pirola C & Cremaschi GA 2006 Integrative study of hypothalamus-pituitary-thyroid-immune system interaction: thyroid hormone-mediated modulation of lymphocyte activity through the protein kinase C signaling pathway. *The Journal of Endocrinology* **189** 45–55. (doi:10.1677/joe.1.06137)

Kuijpens JLP, Nyklíctek I, Louwman MWJ, Weetman T a P, Pop VJM & Coebergh J-WW 2005 Hypothyroidism might be related to breast cancer in post-menopausal women. *Thyroid : Official Journal of the American Thyroid Association* **15** 1253–1259. (doi:10.1089/thy.2005.15.1253)

Li M, Knight DA, Snyder LA, Smyth MJ & Stewart TJ 2013 A role for CCL2 in

674 both tumor progression and immunosurveillance. *OncoImmunology* **2**
675 e25474. (doi:10.4161/onci.25474)
676 Li Z, Qiu Y, Lu W, Jiang Y & Wang J 2018 Immunotherapeutic interventions of
677 Triple Negative Breast Cancer. *Journal of Translational Medicine* **16** 147.
678 (doi:10.1186/s12967-018-1514-7)
679 Linnebacher M & Maletzki C 2012 Tumor-infltrating B cells: The ignored players
680 in tumor immunology. *OncoImmunology* **1** 1186–1188.
681 (doi:10.4161/onci.20641)
682 Maffey A, Storini C, Diceglie C, Martelli C, Sironi L, Calzarossa C, Tonna N,
683 Lovchik R, Delamarche E, Ottobrini L *et al.* 2017 Mesenchymal stem cells
684 from tumor microenvironment favour breast cancer stem cell proliferation,
685 cancerogenic and metastatic potential, via ionotropic purinergic signalling.
686 *Scientific Reports* **7** 13162. (doi:10.1038/s41598-017-13460-7)
687 Mahmoud SM, Paish EC, Powe DG, Macmillan RD, Grainge MJ, Lee AH, Ellis
688 IO & Green AR 2011 Tumor-infiltrating CD8+ lymphocytes predict clinical
689 outcome in breast cancer. *J Clin Oncol* **29** 1949–1955.
690 (doi:10.1200/jco.2010.30.5037)
691 Markowitz J, Wesolowski R, Papenfuss T, Brooks TR & Carson WE 2013
692 Myeloid-derived suppressor cells in breast cancer. *Breast Cancer*
693 *Research and Treatment* **140** 13–21. (doi:10.1007/s10549-013-2618-7)
694 Martin FT, Dwyer RM, Kelly J, Khan S, Murphy JM, Curran C, Miller N,
695 Hennessy E, Dockery P, Barry FP *et al.* 2010 Potential role of
696 mesenchymal stem cells (MSCs) in the breast tumour microenvironment:
697 Stimulation of epithelial to mesenchymal transition (EMT). *Breast Cancer*
698 *Research and Treatment* **124** 317–326. (doi:10.1007/s10549-010-0734-1)

699 Martínez-Iglesias O, García-Silva S, Regadera J & Aranda A 2009
700 Hypothyroidism enhances tumor invasiveness and metastasis
701 development. *PLoS ONE* **4** e6428. (doi:10.1371/journal.pone.0006428)
702 Matilainen H, Yu XW, Tang CW, Berridge M V. & McConnell MJ 2012 Sphere
703 formation reverses the metastatic and cancer stem cell phenotype of the
704 murine mammary tumour 4T1, independently of the putative cancer stem
705 cell marker Sca-1. *Cancer Letters* **323** 20–28.
706 (doi:10.1016/j.canlet.2012.03.028)
707 Melzer C, von der Ohe J & Hass R 2018 Enhanced metastatic capacity of
708 breast cancer cells after interaction and hybrid formation with mesenchymal
709 stroma/stem cells (MSC). *Cell Communication and Signaling* **16** 2.
710 (doi:10.1186/s12964-018-0215-4)
711 Mizejewski GJ 2019 Breast cancer, metastasis, and the microenvironment:
712 disabling the tumor cell-to-stroma communication network. *Journal of*
713 *Cancer Metastasis and Treatment* **5** 35. (doi:10.20517/2394-4722.2018.70)
714 Montesinos M del M & Pellizas C 2019 Thyroid Hormone Action on Innate
715 Immunity. *Frontiers in Endocrinology* **10** 350.
716 (doi:10.3389/fendo.2019.00350)
717 Munn DH & Mellor AL 2006 The tumor-draining lymph node as an immune-
718 privileged site. *Immunological Reviews* **213** 146–158. (doi:10.1111/j.1600-
719 065X.2006.00444.x)
720 Plitas G, Konopacki C, Wu K, Bos PD, Morrow M, Putintseva E V., Chudakov
721 DM & Rudensky AY 2016 Regulatory T Cells Exhibit Distinct Features in
722 Human Breast Cancer. *Immunity* **45** 1122–1134.
723 (doi:10.1016/j.immuni.2016.10.032)

Pottier C, Wheatherspoon A, Roncarati P, Longuespée R, Herfs M, Duray A, Delvenne P & Quatresooz P 2015 The importance of the tumor microenvironment in the therapeutic management of cancer. *Expert Review of Anticancer Therapy* **15** 943–954. (doi:10.1586/14737140.2015.1059279)

Pulaski BA & Ostrand-Rosenberg S 2001 Mouse 4T1 Breast Tumor Model. In *Current Protocols in Immunology*, p Unit 20.2. Hoboken, NJ, USA: John Wiley & Sons, Inc. (doi:10.1002/0471142735.im2002s39)

Ridge SM, Sullivan FJ & Glynn SA 2017 Mesenchymal stem cells: Key players in cancer progression. *Molecular Cancer* **16** 31. (doi:10.1186/s12943-017-0597-8)

Schmohl KA, Müller AM, Wechselberger A, Rühland S, Salb N, Schwenk N, Heuer H, Carlsen J, Göke B, Nelson PJ *et al.* 2015 Thyroid hormones and tetrac: New regulators of tumour stroma formation via integrin αvβ3. *Endocrine-Related Cancer* **22** 941–952. (doi:10.1530/ERC-15-0245)

Schmohl KA, Mueller AM, Dohmann M, Spellerberg R, Urnauer S, Schwenk N, Ziegler SI, Bartenstein P, Nelson PJ & Spitzweg C 2019 Integrin αvβ3-Mediated Effects of Thyroid Hormones on Mesenchymal Stem Cells in Tumor Angiogenesis. *Thyroid* **29** 1843–1857. (doi:10.1089/thy.2019.0413)

Smyth PPA, Shering SG, Kilbane MT, Murray MJ, McDermott EWM, Smith DF & O'Higgins NJ 1998 Serum Thyroid Peroxidase Autoantibodies, Thyroid Volume, and Outcome in Breast Carcinoma. *The Journal of Clinical Endocrinology & Metabolism* **83** 2711–2716. (doi:10.1210/jcem.83.8.5049)

Sogaard M, Farkas DK, Ehrenstein V, Jorgensen JOL, Dekkers OM & Sorensen HT 2016 Hypothyroidism and hyperthyroidism and breast cancer risk: A nationwide cohort study. *European Journal of Endocrinology* **174** 409–414.

749 (doi:http://dx.doi.org/10.1530/EJE-15-0989)
750 van der Spek AH, Fliers E & Boelen A 2017 The classic pathways of thyroid
751 hormone metabolism. *Molecular and Cellular Endocrinology* **458** 29–38.
752 (doi:10.1016/j.mce.2017.01.025)
753 Spitzer MH, Carmi Y, Reticker-Flynn NE, Kwek SS, Madhireddy D, Martins MM,
754 Gherardini PF, Prestwood TR, Chabon J, Bendall SC *et al.* 2017 Systemic
755 Immunity Is Required for Effective Cancer Immunotherapy. *Cell* **168** 487-
756 502.e15. (doi:10.1016/j.cell.2016.12.022)
757 Sterle HA, Valli E, Cayrol F, Paulazo MA, Martinel Lamas DJ, Diaz Flaqué MC,
758 Klecha AJ, Colombo L, Medina VA, Cremaschi GA *et al.* 2014 Thyroid
759 status modulates T lymphoma growth via cell cycle regulatory proteins and
760 angiogenesis. *Journal of Endocrinology* **222** 243–255. (doi:10.1530/JOE-
761 14-0159)
762 Sterle HA, Barreiro Arcos ML, Valli E, Paulazo MA, Méndez Huergo SP, Blidner
763 AG, Cayrol F, Díaz Flaqué MC, Klecha AJ, Medina VA *et al.* 2016 The
764 thyroid status reprograms T cell lymphoma growth and modulates immune
765 cell frequencies. *Journal of Molecular Medicine* **94** 417–429.
766 (doi:10.1007/s00109-015-1363-2)
767 Sterle HA, Nicoud MB, Massari NA, Táquez Delgado MA, Herrero Ducloux MV,
768 Cremaschi GA & Medina VA 2019 Immunomodulatory role of histamine H4
769 receptor in breast cancer. *British Journal of Cancer* **120** 128–138.
770 (doi:10.1038/s41416-018-0173-z)
771 Szychta P, Szychta W, Gesing A, Lewiński A & Karbownik-Lewińska M 2013
772 TSH receptor antibodies have predictive value for breast cancer -
773 Retrospective analysis. *Thyroid Research* **6** 8. (doi:10.1186/1756-6614-6-8)

774 Tang HY, Lin HY, Zhang S, Davis FB & Davis PJ 2004 Thyroid hormone causes
775 mitogen-activated protein kinase-dependent phosphorylation of the nuclear
776 estrogen receptor. *Endocrinology* **145** 3265–3272. (doi:10.1210/en.2004-
777 0308)
778 Tosovic A, Bondeson A-G, Bondeson L, Ericsson U-B, Malm J & Manjer J 2010
779 Prospectively measured triiodothyronine levels are positively associated
780 with breast cancer risk in postmenopausal women. *Breast Cancer*
781 *Research* **12** R33. (doi:10.1186/bcr2587)
782 Vikas P, Borcherding N & Zhang W 2018 The clinical promise of
783 immunotherapy in triple-negative breast cancer. *Cancer Management and*
784 *Research* **10** 6823–6833. (doi:10.2147/CMAR.S185176)
785 Weng C-H, Chen Y-H, Lin C-H, Luo X & Lin T-H 2018 Thyroid disorders and
786 breast cancer risk in Asian population: a nationwide population-based
787 case-control study in Taiwan. *BMJ Open* **8** 20194. (doi:10.1136/bmjopen-
788 2017-020194)
789 Yoshimura T, Howard OMZ, Ito T, Kuwabara M, Matsukawa A, Chen K, Liu Y,
790 Liu M, Oppenheim JJ & Wang JM 2013 Monocyte chemoattractant protein-
791 1/CCL2 produced by stromal cells promotes lung metastasis of 4T1 murine
792 breast cancer cells. *PloS One* **8** e58791.
793 (doi:10.1371/journal.pone.0058791)
794
795

Figure Legends

Figure 1: **Modulation of breast tumor growth and dissemination by thyroid status.** Euthyroid (control), hyperthyroid (hyper) and hypothyroid (hypo) Balb/c mice were orthotopically inoculated with $1x10^5$ 4T1 cells. **(A)** Time-course increase in tumor volume among the three experimental groups (n=6 mice per group). **(B)** Tumor weight at days 21 and 35 post inoculation (p.i.) of tumor cells (n=6-9 mice per group). **(C)** Representative images of tumors at day 35 p.i. **(D)** Number of metastatic foci in lungs at day 35 p.i. (n=7-9 mice per group). **(E)** Representative images of lungs at day 35 p.i., black arrows indicate metastatic foci. **(F)** Number of metastatic foci in lungs after 35 days of i.v. injection of $1x10^5$ 4T1 cells (n=5 mice per group). **(G)** Plasmatic levels of thyroid hormones in euthyroid, hyperthyroid, and hypothyroid mice at 21 and 35 days p.i., determined using RIA and of TSH determined by ELISA (n=6-9 mice per group). Results are the mean ± SEM. Means differ with *p<0.05, **p<0.05, ***p<0.05.

Figure 2: Histopathological analysis and evaluation of cell proliferation and apoptosis in 4T1 tumors. (A) Representative images of H&E staining and PCNA and TUNEL immunostaining of tissue sections of paraffin-embedded tumors from control, hyper- and hypothyroid mice (×400 original magnification, Scale bar = 20 µm). **(B)** Percentage of necrotic areas and PCNA-positive cells per field and number of TUNEL-positive cells per field at ×400 magnification in 10 random fields (n=3-4 mice per group). 4T1 cells were starved for 24 h and then treated with or without the combination of thyroid hormones (THs) at physiologic (T3 $1x10^{-9}$ mol/L, T4 $1x10^{-7}$ mol/L) or supraphysiologic (T3 $1x10^{-8}$

820 mol/L, T4 $1x10^{-6}$ mol/L) levels for 24h. **(C)** Cell viability relative to physiologic
821 levels of T3 and T4 (control) was evaluated by Cell Titer Blue assay. **(D)** Cell
822 proliferation was evaluated by BrdU incorporation assay and analyzed by flow
823 cytometry; median fluorescence intensity (MFI); **(E)** representative histograms.
824 Results are the mean ± SEM of three independent experiments. Means differ
825 with *p<0.05, **p<0.01 or ***p<0.001.

826 **Figure 3: Distribution of tumor-infiltrating immune cell subsets.** Flow
827 cytometry analysis was performed on cell suspensions obtained from tumors
828 from euthyroid (control), hyperthyroid (hyper) and hypothyroid (hypo) mice at 21
829 and 35 days post inoculation (p.i.). Percentage **(A)** and representative dot plots
830 **(B)** of tumor infiltrating lymphocytes (TILs) obtained by forward vs. side scatter
831 analysis. Percentage of **(C)** NK cells; **(D)** $CD19^+$ B lymphocytes; **(E)** $CD4^+$ T
832 helper cells; **(F)** $CD8^+$ T cytotoxic lymphocytes or **(G)** activated $CD8^+$ T cytotoxic
833 lymphocytes within the TIL-gated population. **(H)** Percentage of MDSC
834 infiltrating cells. Results are the mean ± SEM of n=7-9 mice per group. Means
835 differ with *p<0.05 or **p<0.01.

836 **Figure 4: Cytokine production by 4T1 tumors.** Tumors from euthyroid
837 (control), hyperthyroid (hyper) and hypothyroid (hypo) mice were excised 35
838 days post inoculation (p.i.), cut into small pieces and incubated during 24h in
839 DMEM at 37°C to obtain tumor conditioned media (CM). The concentration of
840 **(A)** IFNγ, **(B)** IL-10, **(C)** the ratio between IFNγ and IL-10, **(D)** TNFα and **(E)**
841 CCL2, was quantified in the CM using the CBA method. Results are the mean ±
842 SEM of n=6 mice per group. Means differ with *p<0.05.

843 **Figure 5: Distribution of spleen immune cell subsets.** Euthyroid (control),

hyperthyroid (hyper) and hypothyroid (hypo) mice were orthotopically inoculated with 4T1 cells. Splenocytes were obtained at the indicated time points post-inoculation (p.i.) and stained with specific antibodies for **(A)** NK cells; **(B)** B lymphocytes; **(C)** cytotoxic T lymphocytes; **(D)** activated cytotoxic T lymphocytes, **(E)** myeloid-derived suppressor cells or **(F)** regulatory T cells and analyzed by flow cytometry. Splenocytes from 35-day tumor bearing mice were co-cultured during 24h with irradiated 4T1 cells in DMEM at 37°C to obtain conditioned media (CM). The concentration of **(G)** IFNγ and **(H)** IL-10 was quantified by ELISA and **(I)** the ratio between IFNγ and IL-10 levels was calculated. Results are the mean ± SEM of n=6-9 mice per group. Means differ with *p<0.05, **p<0.01 or ***p<0.001.

Figure 6: Migration of BM-derived MSCs to tumors and lungs. Euthyroid (control), hyperthyroid (hyper) and hypothyroid (hypo) Balb/c mice were orthotopically inoculated with 4T1-fluc cells. After 28 days DiR stained BM-MSC were intravenous (i.v.) inoculated. After 7 days tumors, lungs, spleens and livers were obtained and analyzed by *ex vivo* imaging. **(A)** Representative images of the radiant efficiency of DiR prelabeled MSC in tumors. **(B)** Ratio between DiR fluorescence and luciferase luminescence in tumors. **(C)** Representative images of the radiant efficiency of DiR prelabeled MSC in lungs (highlighted with a white circle) and spleens and livers as control. **(D)** Ratio between DiR fluorescence and luciferase luminescence in lungs. Results are the mean ± SEM of n=4 mice per group. The migration of BM-MSC towards conditioned media (CM) obtained from **(E)** tumors 35 days post inoculation (p.i.) or **(F)** lungs

35 days p.i. was analyzed using the Boyden chamber assay; the number of cells attached to the bottom of the membrane is shown. Basal cell migration was evaluated using DMEM 5% FBS instead of CM. Results are the mean ± SEM of n=8 mice per group. BM-MSC were cultured in complete medium supplemented or not (Basal) with 10% CM obtained from tumors 35 days p.i. Representative images of the cells stained with crystal violet **(G)** and the calculated cell areas **(H)** are shown. Scale bar= 100µm. Results are the mean ± SEM of n=3 mice per group. Means differ with *$p<0.05$ or **$p<0.01$.

Figure 1

A

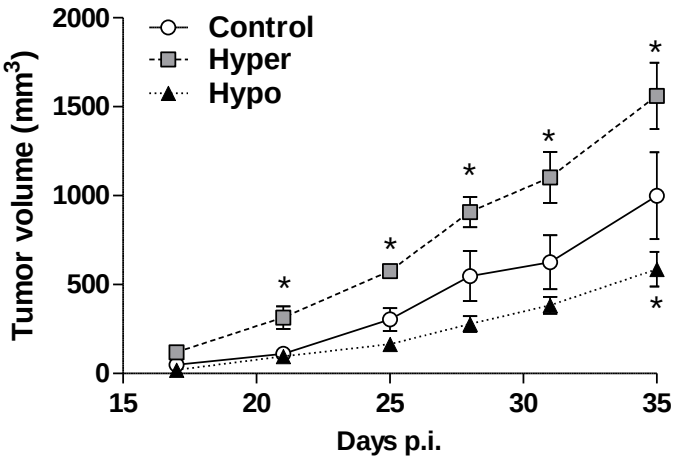

B

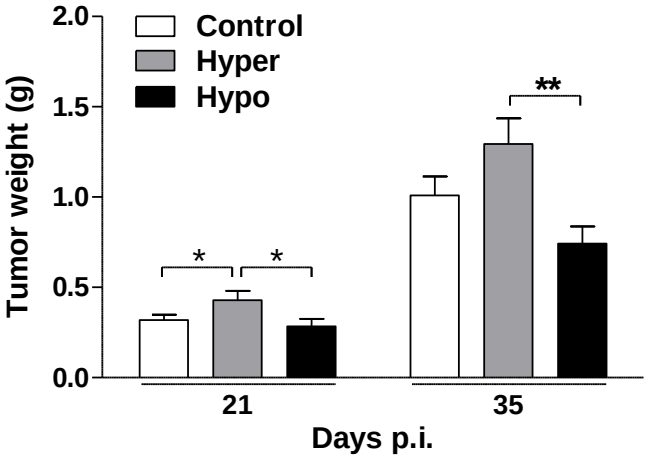

C

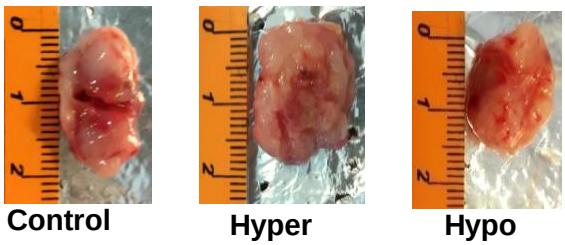

D

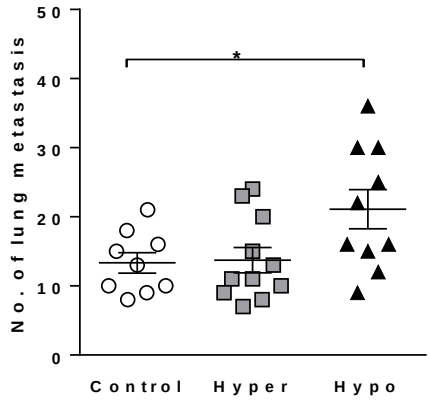

E

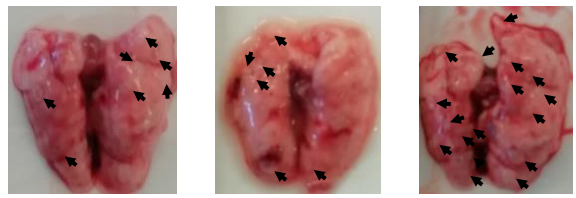

F

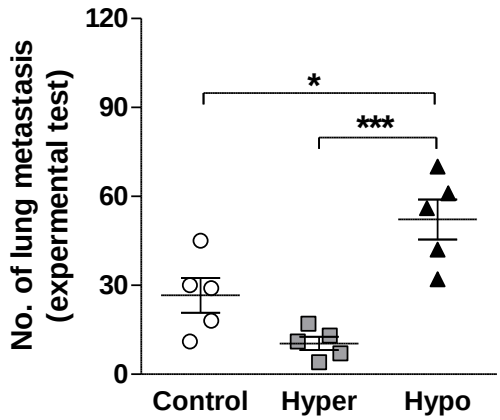

G

	21 days			35 days		
	Euthyroid	Hyperthyroid	Hypothyroid	Euthyroid	Hyperthyroid	Hypothyroid
T3 (ng/dl)	105 ± 7	343 ±45*	62 ± 8*	87 ± 12	372 ±41*	47 ± 6*
T4 (μg/dl)	4.3 ± 0.8	18.4 ± 1.8*	< 1	4.0 ± 1.2	20.3 ± 1.7*	< 1
TSH (ng/ml)	45±4	< 20	80±7*	48±6	< 20	76±10*

Figure 2

A

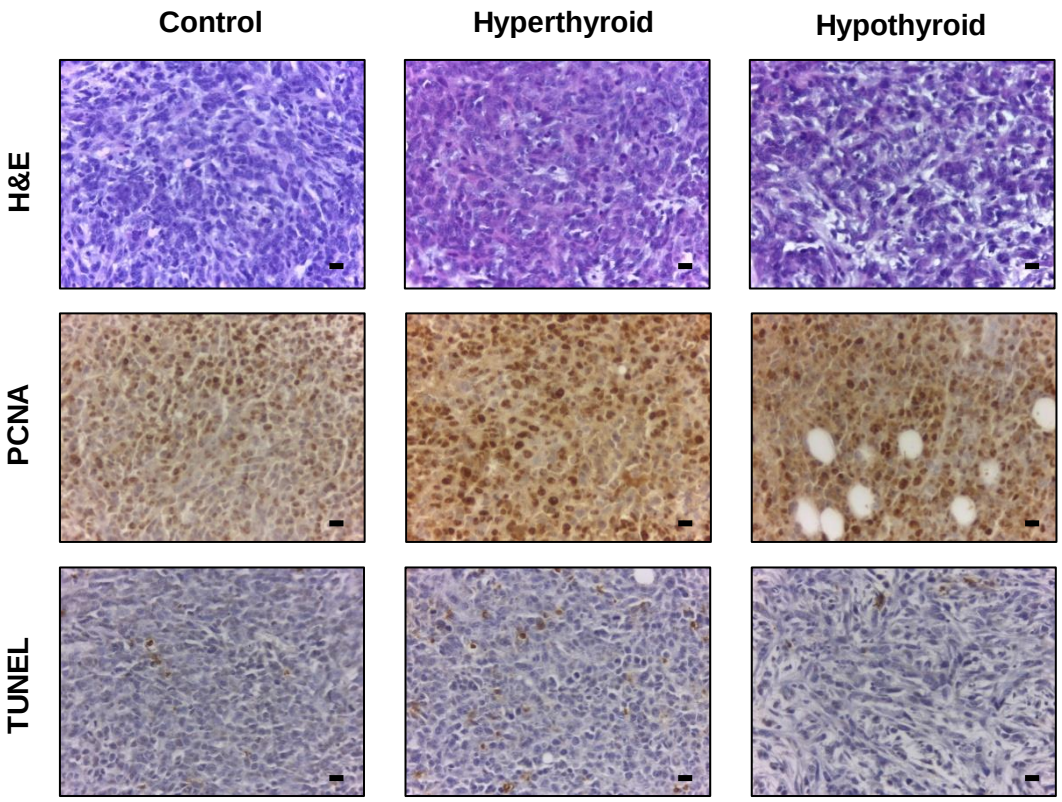

B

	Control	Hyperthyroid	Hypothyroid
Necrosis (%)	57 ± 6	55 ± 7	70 ± 8
PCNA-positive cells (%)	75 ± 11	80 ± 13	56 ± 15
Tunel-positive cells per field	1.8 ± 0.9	3.0 ± 1.3	2.0 ± 0.8

C

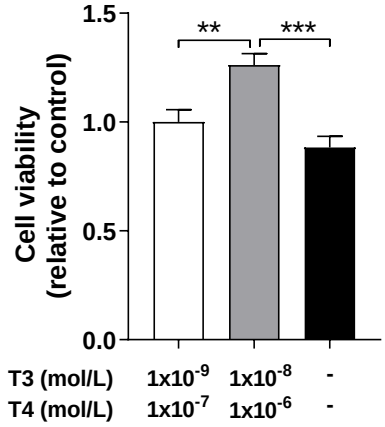

D

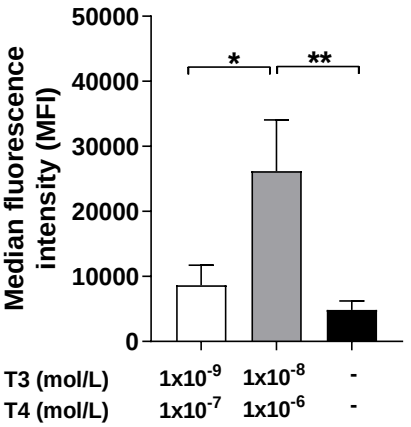

E

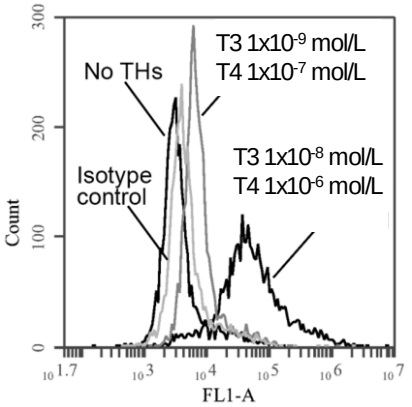

Figure 3

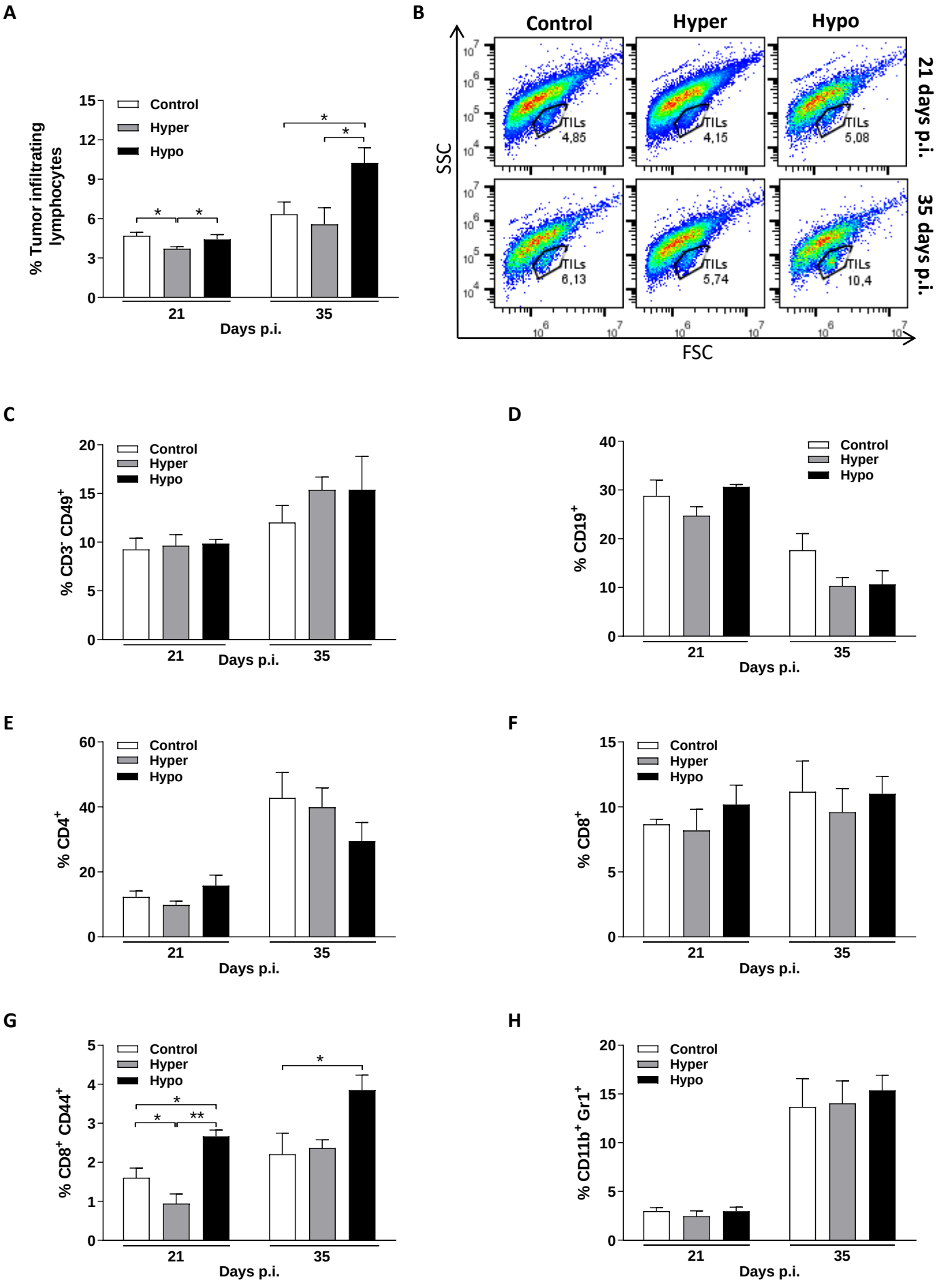
A
% Tumor infiltrating lymphocytes
Control
Hyper
Hypo
Days p.i.
21
35
B
Control
Hyper
Hypo
21 days p.i.
35 days p.i.
TILs 4,85
TILs 4,15
TILs 5,08
TILs 6,13
TILs 5,74
TILs 10,4
SSC
FSC
C
% CD3- CD49+
D
% CD19+
E
% CD4+
F
% CD8+
G
% CD8+ CD44+
H
% CD11b+ Gr1+

Figure 4

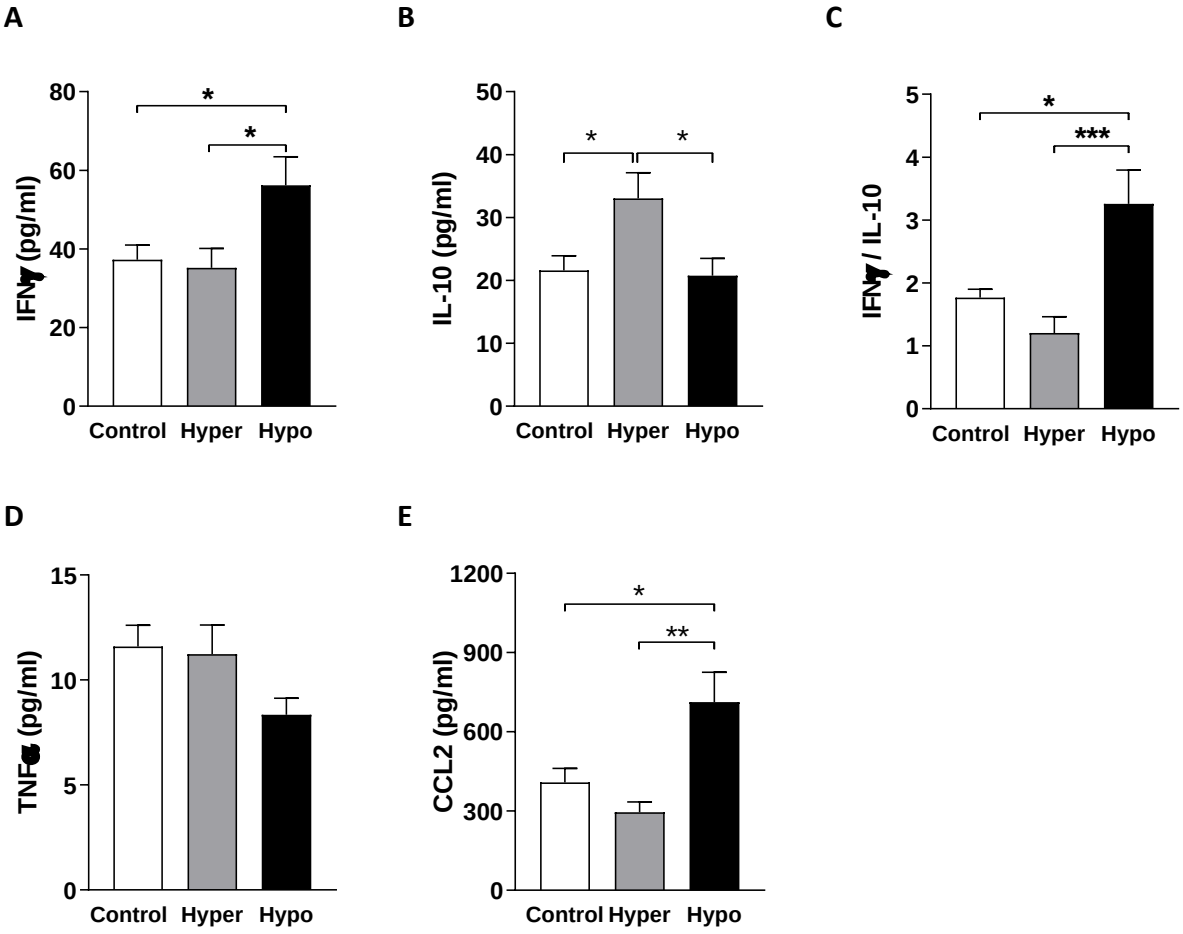
A
B
C
D
E
IFNγ (pg/ml)
IL-10 (pg/ml)
IFNγ / IL-10
TNFα (pg/ml)
CCL2 (pg/ml)
Control
Hyper
Hypo
*
**
***

Figure 5

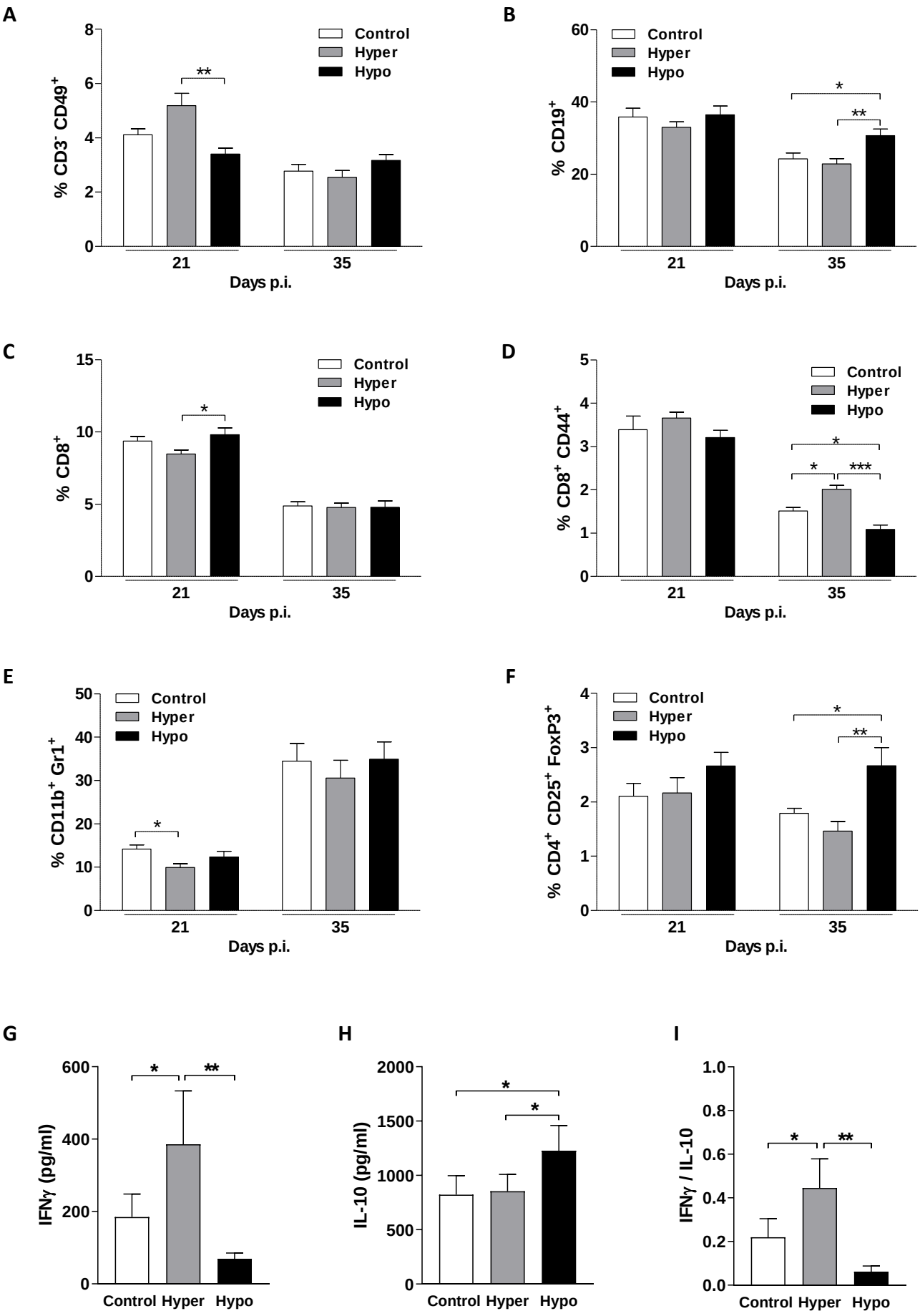
A
% CD3- CD49+
Control
Hyper
Hypo
Days p.i.
B
% CD19+
C
% CD8+
D
% CD8+ CD44+
E
% CD11b+ Gr1+
F
% CD4+ CD25+ FoxP3+
G
IFNγ (pg/ml)
H
IL-10 (pg/ml)
I
IFNγ / IL-10

Figure 6

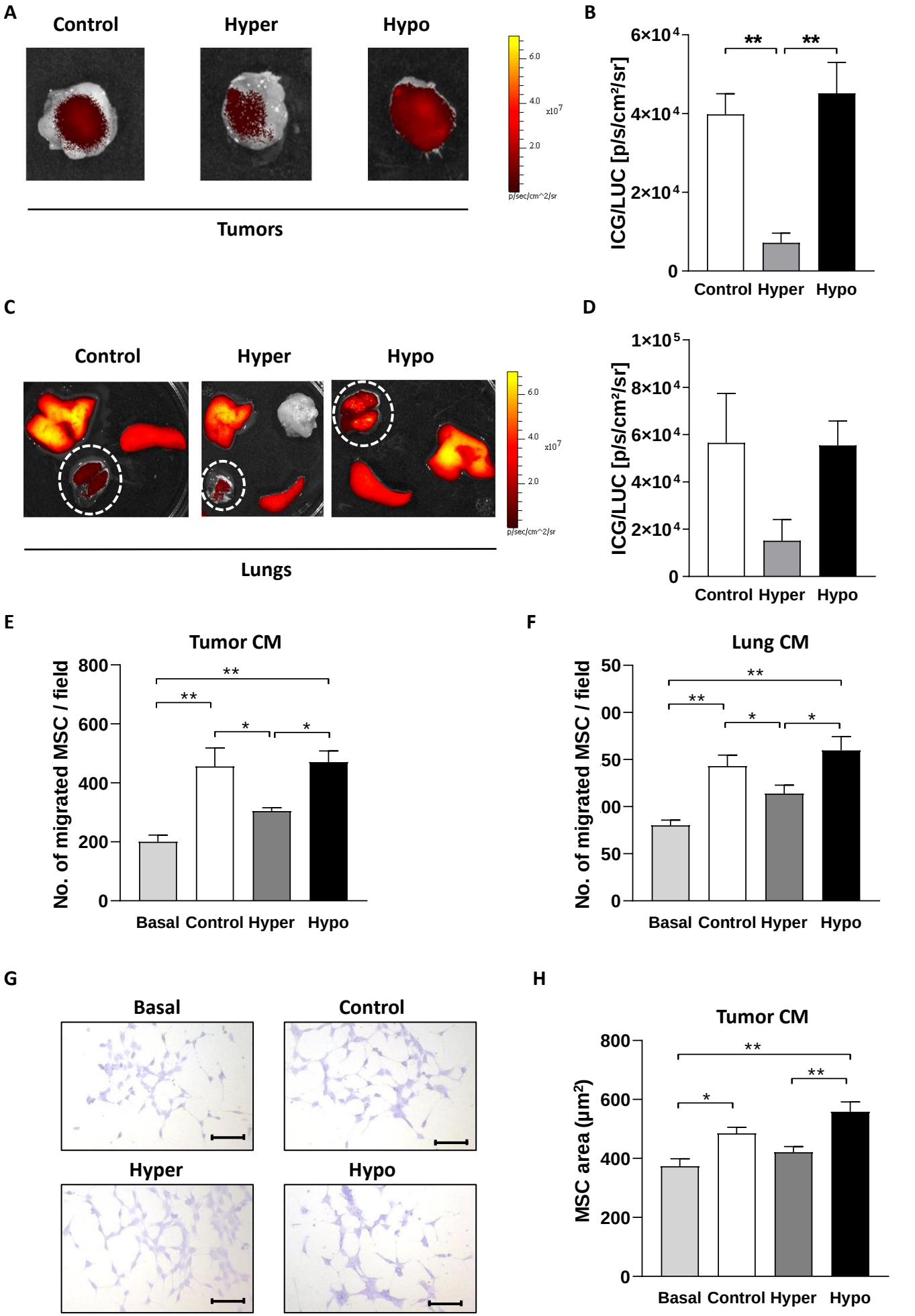
A
Control
Hyper
Hypo
6.0
4.0
x10^7
2.0
p/sec/cm^2/sr
Tumors
B
6×10^4
4×10^4
2×10^4
0
**
**
ICG/LUC [p/s/cm²/sr]
Control Hyper Hypo
C
Control
Hyper
Hypo
6.0
4.0
x10^7
2.0
p/sec/cm^2/sr
Lungs
D
1×10^5
8×10^4
6×10^4
4×10^4
2×10^4
0
ICG/LUC [p/s/cm²/sr]
Control Hyper Hypo
E
Tumor CM
800
600
400
200
0
No. of migrated MSC / field
**
**
*
*
Basal Control Hyper Hypo
F
Lung CM
50
00
50
00
50
0
No. of migrated MSC / field
**
**
*
*
Basal Control Hyper Hypo
G
Basal
Control
Hyper
Hypo
H
Tumor CM
800
600
400
200
0
MSC area (µm²)
**
**
*
Basal Control Hyper Hypo

Supplementary Materials and Methods

Cell culture

The tumor cell line 4T1 (ATCC CRL-2539) was cultured and maintained in Dulbecco's Modified Eagle Medium (DMEM) supplemented with 10% v/v FBS, 0.03% w/v glutamine, 0.01% w/v streptomycin, and 100 U/ml penicillin (all from Gibco, Grand Island, NY, USA). Cells were maintained at 37 °C in a humidified atmosphere containing 5% CO_2 (Sterle *et al.* 2019).

Proliferation assays

To analyze the effects of THs *in vitro*, cells were serum-deprived for 24h and then treated with the combination of physiologic concentrations of both triiodothyronine (T3, $1x10^{-9}$ mol/L; Sigma-Aldrich, MO, USA) and L-thyroxine (T4, $1x10^{-7}$ mol/L; Sigma-Aldrich), supraphysiologic concentrations of T3 and T4 ($1x10^{-8}$ mol/L and $1x10^{-6}$ mol/L, respectively) or none THs for additional 24h, to mimic euthyroid, hyperthyroid and hypothyroid conditions, respectively. Cells were incubated for the last 2h with $3x10^{-5}$ mol/L 5-bromo-2'-deoxyuridine (BrdU; Sigma-Aldrich) and fixed with 70% v/v cold ethanol for 30min. To perform DNA denaturation, cells were incubated with HCl 2N for 30min and then washed with $Na_2B_4O_7$ 0.1 mol/L. Finally, cells were incubated with an antibody against BrdU (Sigma-Aldrich) and an Alexa 488-conjugated secondary antibody (Sigma-Aldrich). Samples were run on a BD Accuri C6 flow cytometer (BD Biosciences, CA, USA) and data was analyzed using the BD Accuri C6 software (BD Biosciences). Alternatively, the fluorometric resazurin reduction method (CellTiter-Blue; Promega, WI, USA) was used (Cayrol *et al.* 2015). For this, cells were incubated for the last 30min with the reactive and the fluorescence was determined in a BMG Labtech NOVOstar MicroPlate Reader. Fluorescence

was determined for 6 replicates per treatment condition, and cell proliferation in THs-treated cells was normalized to their respective control.

Hormone determinations

Blood was collected from the tail vein and serum was obtained by centrifugation. T3 and T4 serum levels were determined using commercial RIA kits (Immunotech, Prague, Czech Republic) according to the manufacturer's instructions. The serum levels of TSH were assayed using an ELISA kit (Uscn Life Science, Inc., Wuhan, Hubei, Republic of China) (Sterle *et al.* 2016).

Histochemistry and immunostaining

Tumors were excised, fixed in 4% (v/v) formaldehyde in PBS, paraffin-embedded and sliced into 4-µm thick sections. The histological characteristics were evaluated on haematoxylin–eosin (H&E)-stained specimens (Biopur diagnostic, Buenos Aires, Argentina).

Immunohistochemistry was performed using the primary mouse anti-proliferating cell nuclear antigen (PCNA) antibody (1:100, clone PC10, Dako Cytomation, Denmark). The fragmented DNA was detected by using Apoptag^{TM} plus peroxidase in situ apoptosis Detection Kit (Millipore, MA, USA) according to the manufacturer's instructions. Analysis of samples was performed with an optical microscope Leica ICC50 HD (Wetzlar Germany), and photographs were taken at × 400 magnification with Leica camera (Germany) and visualized with the Leica LAS EZ software (version 3.1.0, Leica Microsystem, Switzerland).

Preparation of single cell suspensions from lymph nodes, spleens and tumors

Lymphoid organs and solid tumors were removed and disrupted through a 1-mm metal mesh. The red blood cells were lysed using a buffer containing 0.15 mol/L NH_4Cl, 0.01 mol/L K_2CO_3 and $1x10^{-4}$ mol/L EDTA. The resulting cell suspensions were filtered through a 40-µm cell strainer (BD Biosciences) and resuspended in PBS.

Cytokine determination

Tumors and spleens were obtained from mice 35 days post-tumor inoculation (p.i.). Tumors were cut in small pieces and equal quantities of tissue were incubated in complete DMEM medium. Spleens were disrupted through a 1-mm metal mesh and seeded at a final concentration of $1×10^7$ cells/ml in complete DMEM medium and co-incubated with 4T1 irradiated cells (30 Gy) at a ratio 10:1. The conditioned medium was obtained after 24 h. Mice interferon (IFN)-γ, tumor necrosis factor (TNF), interleukin (IL)-10 and chemokine (C-C motif) ligand (CCL)-2 CBA Flex Sets (BD Biosciences) were used to quantify specific cytokines in a BD Accuri C6 flow cytometer, following the manufacturers' instructions. Results were analyzed with FCAP Array Software v3.0 (BD Biosciences). Alternatively, IFN-γ and IL-10 levels were quantified using ELISA (Invitrogen, CA, USA) following the manufacturers' instructions. The absorbance analysis was performed at 450 nm with the Multiskan GO Microplate Spectrophotometer (Thermo Scientific, MA, USA).

MSC morphology analysis

Tumor conditioned media (CM) were obtained as described. MSC were cultured with complete medium and 10% CM from control, hyper or hypo mice. Complete medium alone was used as a negative control. After 7 days, cells were washed twice with PBS and fixed with ice-cold methanol, and then stained with crystal violet 0.01% w/v. Cells were mounted (mounting medium and

coverglass) and visualized under Nikon Eclipse E400 microscope (USA). Three photographs were taken per condition at x100 magnification. At least 20 individual cells were selected and cell surface area was measured with Image J software (NIH, National Institutes of Health).

Supplementary References

Cayrol F, Díaz Flaqué MC, Fernando T, Yang SN, Sterle HA, Bolontrade M, Amorós M, Isse B, Farías RN, Ahn H *et al.* 2015 Integrin αvβ3 acting as membrane receptor for thyroid hormones mediates angiogenesis in malignant T cells. *Blood* **125** 841–851. (doi:10.1182/blood-2014-07-587337)

Colombo LL, Vanzulli SI, Villanueva A, Cañete M, Juarranz A & Stockert JC 2005 Long-term regression of the murine mammary adenocarcinoma, LM3, by repeated photodynamic treatments using meso-tetra (4-N-methylpyridinium) porphine. *International Journal of Oncology* **27** 1053–1059. (doi:10.3892/ijo.27.4.1053)

Supplementary Figure 1

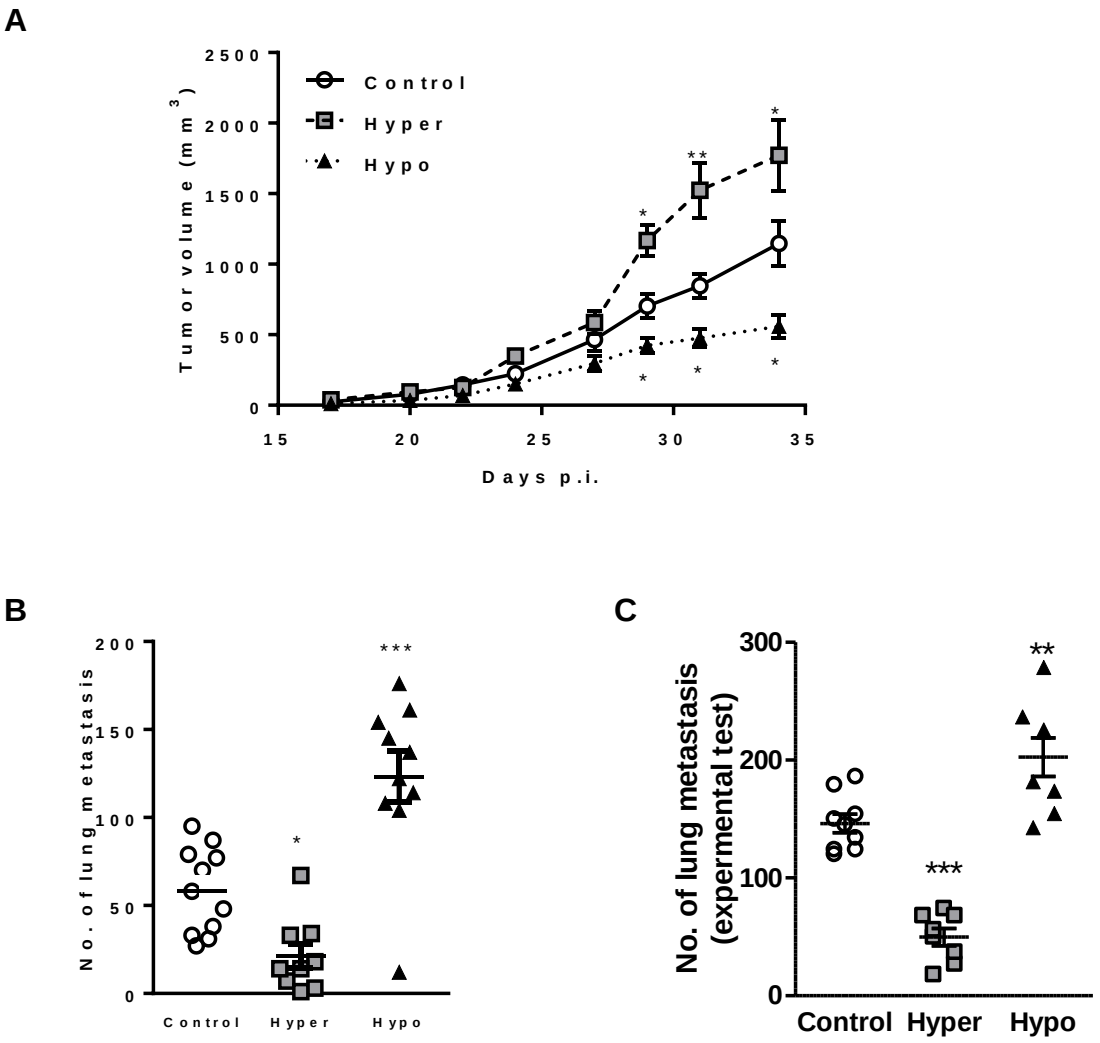

Modulation of LM3 breast tumor growth and dissemination by thyroid status. Euthyroid (control), hyperthyroid (hyper) and hypothyroid (hypo) Balb/c mice were orthotopically inoculated with $1x10^5$ LM3 cells (from a Balb/c mammary adenocarcinoma) (Colombo *et al.* 2005), as described in the "*materials and methods"* section. **(A)** Time-course increase in tumor volume among the three experimental groups (n=9-11 mice per group). **(B)** Number of metastatic *foci* in lungs at day 40 post inoculation (p.i.) (n=9-11 mice per group). **(C)** Number of metastatic *foci* in lungs after 40 days of intravenous (i.v.) injection of $1x10^5$ LM3 cells (n=7-8 mice per group).

Supplementary Figure 2

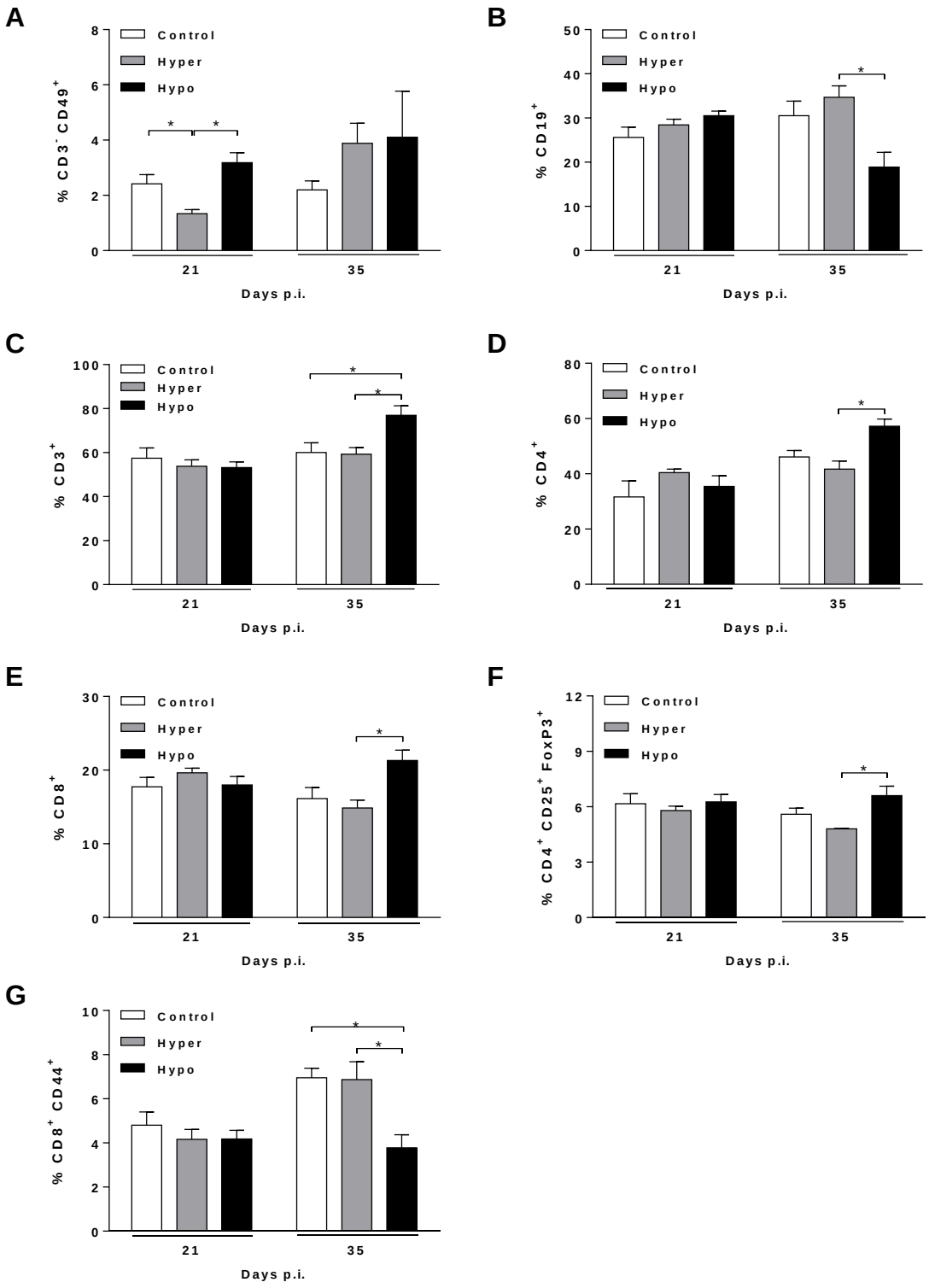

Distribution of immune subsets in tumor-draining lymph nodes (TDLN). Euthyroid (control), hyperthyroid (hyper) and hypothyroid (hypo) mice were orthotopically inoculated with 4T1 cells. Cell suspensions were obtained from TDLN at the indicated time points post-inoculation (p.i.) and stained with specific antibodies for **(A)** NK cells; **(B)** B lymphocytes; **(C)** T lymphocytes; **(D)** T helper lymphocytes; **(E)** cytotoxic T lymphocytes; **(F)** regulatory T lymphocytes or **(G)** activated cytotoxic T lymphocytes. Results are the mean ± SEM of n=5-6 mice per group. Means differ with *p<0.05